Hydronium and hydroxide at the interface between water and hydrophobic media

Robert Vácha[1], Dominik Horinek,[2*] Max L. Berkowitz[3] and Pavel Jungwirth[1*]

[1]*Institute of Organic Chemistry and Biochemistry, Academy of Sciences of the Czech Republic and Center for Biomolecules and Complex Molecular Systems, Flemingovo nám. 2, 16610 Prague 6, Czech Republic.*

[2]*Physik Department, Technische Universität München, 85748 Garching, Germany*

[3]*Department of Chemistry, University of North Carolina,Chapel Hill, North Carolina 27599, USA*

*Corresponding authors. E-mails: dominik.horinek@ph.tum.de (D.H.) and pavel.jungwirth@uochb.cas.cz (P. J.).

Abstract

The behavior of hydronium and hydroxide ions at the water/alkane, water/vapor and water/rigid wall interfaces was investigated by means of molecular dynamics simulations. All these interfaces exhibit a strong affinity for hydronium, which is in agreement with spectroscopic and low pH zeta-potential measurements. Except for the water/rigid wall interface, which strongly structures water and weakly attracts OH^-, none of the other investigated interfaces shows an appreciable acumulation of hydroxide. This computational result is at odds with the interpretation of higher pH zeta-potential and titration experiments, however, it is supported by surface selective spectroscopies of the surface of water and hydroxide solutions.

Introduction

With the advent of surface selective spectroscopic techniques, combined with large scale molecular simulations, there has been a renewed interest in the detailed molecular structure of aqueous interfaces.[1] In particular, significant attention has been paid to specific interfacial affinities of ions of simple salts such as alkali halides.[2-8] But even in the pure liquid without any salt there are still ions present due to the remarkable ability of water to autoionize (autolyze), which results in the formation of hydronium and hydroxide. While in bulk water the concentration of these ions is very low (10^{-7} mol/l in pH neutral liquid), interfacial enhancement has been invoked in many recent studies discussed in detail in the next paragraphs. Interestingly and somewhat controversially, researchers agree neither on the quantitative degree of this enhancement nor on which of the two ions, H_3O^+ or OH^-, exhibits a larger affinity for aqueous interfaces.[9-11]

Calculations involving the surface of water, as well as acid and base solutions, show an appreciable surface enhancement of hydronium but not of hydroxide. Different computational techniques, ranging from classical force field molecular dynamics (MD), over the Effective Valence Bond (EVB) method, to ab initio MD predict surface affinity of hydronium expressed in terms of either increased surface concentration by about one or two orders of magnitude or surface free energy minimum of up to several kcal/mol.[12-16] A semi-quantitative explanation of the surface propensity of hydronium lies in the low negative charge of the oxygen of the cation which makes it a poor hydrogen bond acceptor. H_3O^+ can thus stabilize at the water surface with its oxygen pointing into the gas phase and the three hydrogens forming strong hydrogen bonds to neighboring water molecules. It is from this perspective that hydronium has been labeled as the smallest amphiphilic species.[12] For a fully quantitative picture, one has to take also into account that the hydrated proton interconverts fast between the two limiting structures of an Eigen (H_3O^+ with three strongly hydrogen-

bonded water molecules)[17] and Zundel ($H_5O_2^+$)[18] cations. In contrast to hydronium, neither classical nor ab initio MD simulations show an appreciable affinity of hydroxide for water surface.[14,16] OH^- can occasionally penetrate all the way to the surface with its hydrogen pointing into the gas phase, however, it does not accumulate there. This can be rationalized by the fact that the hydrogen of OH^-, albeit weakly hydrated, still bears a large enough positive charge to form a weak donating hydrogen bond.[19-21] The amphifilic character of hydroxide is thus weaker than that of hydronium.

These computational results are supported by surface sensitive spectroscopic measurements. Vibrational sum frequency generation (VSFG) spectroscopy of acid and base solutions of varying concentration show a strong effect of hydronium but not of hydroxide on the spectra of the interfacial aqueous layer.[2,14,22] Second harmonic generation (SHG) spectroscopy of solutions with concentrations of hydronium or hydroxide varying from milimolar to molar range indicate increased affinity of H_3O^+ for the surface, while for OH^- the best fit to the data implies a weak repulsion of this anion from the surface.[23-25] A similar picture is also born out from IR measurements of solid aqueous nanoparticles.[16] In addition, photoelectron spectroscopy (PES) of pure water and NaOH solutions of varying concentrations does not reveal surface adsorption of hydroxide.[3,26]

In contrast to the above computational and spectroscopic findings, numerous studies by colloid chemists and electrochemists show accumulation of a negative charge at aqueous interfaces, which has been mostly interpreted in terms of surface adsorption of OH^-. Negative charge has been observed on small water droplets (the so called waterfall effect) and air bubbles in water, as well as on oil droplets in water, where titration curves have been also measured.[27-34] In addition, hydroxide adsorption has been invoked for rationalizing the stability of thin aqueous films.[35-37]

The colloid science experiments are typically exploring the water/oil rather than the water/vapor interface, which raises the question of the possibly different behavior of the ionic product of water at these interfaces. In this context it is worth mentioning that MD simulations of the water/diamond interface revealed a shallow (<0.5 kcal/mol) free energy minimum for hydroxide about 5 Å from the surface carbon layer[38] and, similarly, simulations of water next to a hard wall with a strong dispersion ingteraction to water showed accumulation of OH^- in the vicinity of the interface.[39] A most recent simulation study demonstrated that this accumulation is due to the rather special properties (hardness and strength of the van der Waals attraction to water) of the employed carbon-like wall and that the interfacial OH^- peak all but disappears for softer and less attractive model hydrophobic environments.[40] The principle aim of the present study is to explore surface behavior of hydroxide and hydronium at realistic interfaces between water and long chain alkane hydrophobic phases using MD simulations. This allows us to address quantitatively the question of the relation between water/oil and water/vapor interfaces in terms of surface segregation of the ionic product of water with the aim of narrowing the existing controversy concerning the interfacial behavior of hydronium and hydroxide.

Methods

By means of MD simulations in extended slab geometries we investigated the behavior of hydronium and hydroxide at four different water/hydrophobic medium interfaces: i) water/disordered decane ($C_{10}H_{22}$) or icosane ($C_{20}H_{42}$), ii) water/ordered decane, iii) water/rigid wall, and iv) water/vapor. These four interfaces are depicted as snapshots from MD simulations in Figure 1. Sufficiently long simulations were performed in order to obtain the density profiles of a single H_3O^+ or OH^- ion along the z-coordinate perpendicular to the interface. In addition, we also evaluated potentials of mean force, i.e., free energy profiles

along the z-coordinate of the water/icosane interface, separately for hydronium and hydroxide.

The unit cells for simulations with periodic boundary conditions of water/decane interfaces contained 723 waters and 64 decane molecules generated in two different initial configurations. The first one denoted as the water/ordered decane interface was generated with aliphatic chains in all-trans conformations closely packed along the z-coordinate leading to a dense ordered layer next to water with a unit cell of approximately 35 x 35 x 34 Å. To create the second configuration, i.e., the water/disordered decane system, an ordered layer of decane was first heated at constant volume to 400 K and, after 2 ns, it was cooled back to 300 K. This, now disordered layer of decane was placed next to water and additional 2 ns of an equilibration run at constant temperature and pressure were carried out. This yielded a water/disordered decane interface with a unit cell of roughly 24.4 x 24.4 x 72.2 Å. Production runs for both systems were performed at 300 K and 1 atm.

For comparison, we investigated two additional interfaces between water and a hydrophobic medium. One, denoted as water/rigid wall interface is formed by two hydrophobic carbons walls, each consisting of 418 carbon-like atoms placed in a close packed layer, between which 1960 water molecules were placed, similarly as in our previous study.[40] Application of periodic boundary conditions to the unit cell of 42 x 43 x 100 Å led to an extended water slab confined by two rigid carbon-like walls. The system evolved at 300 K (except for the carbon-like atoms which were kept frozen). Finally, a water/vapor interface was modeled by placing 723 water molecules in prismatic cell of dimensions 24 x 24 x 272 Å. Employing periodic boundary conditions yielded in infinite water slab with two water/vapor interfaces.

Next, we inserted in each of the above four systems a single H_3O^+ or OH^- ion together with its counter ion (Cl^- or Na^+). All these MD simulations were performed with a polarizable

force field employing the program package Gromacs (version 3.3.1) compiled in double precision.[41] Production runs of 20 ns were performed with a time step of 1 fs. A Lennard-Jones interaction cutoff of 11 Å was employed. The long range electrostatic interactions were accounted for via the Particle Mesh Ewald (PME) method.[42] For water we used the POL3 model,[43] while polarizable force fields for H_3O^+ and OH^- were taken from our previous work.[9] Parameters (including polarizabilities) for decane were derived from the General Amber Force Field (GAFF)[44] for which the partial charges were evaluated using the standard RESP procedure after a Hartree-Fock calculation with the 6-31g* basis set and fitting the electrostatic potential at points selected according to the Merz-Singh-Kollman scheme.[45] The rigid wall was constructed from neutral carbon-like atoms with the same Lennard-Jones parameters as in previous studies.[39,40]

The present polarizable force field for H_3O^+ or OH^- reproduces benchmark ab initio energetics and structures of small water-ion clusters.[9] For hydrated proton, parameters were developed and tested for both Eigen and Zundel cations and similar surface affinities were observed for these two limiting cases.[9] Therefore, in this study we focused only on the more abundant Eigen form of hydronium. Classical force field cannot in principle describe proton hopping which, however, does not qualitatively change the equilibrium partitioning of hydronium between the interface and the bulk.[9]

Our hydroxide oxygen hydrogen-binds in the bulk liquid on average five water molecules, while ab initio MD simulations and X-ray diffraction measurements predict a number between four and five[19,20] and neutron diffraction deduces about four accepting hydrogen bonds or slightly less.[46] In agreement with these studies the present OH^- also donates about one additional weak hydrogen bond. The present polarizable force field for hydroxide thus performs better than a non-polarizable one, which was critically tested recently.[20] The advantage of a polarizable potential is that it can at least to some extent

account for the partially charge-transfer character of the strong HOH-OH^- hydrogen bond. Nevertheless, we performed an additional "stability check" of the hydroxide force field varying the partial charges on H and O atoms (by up to -0.15 e) or the Lennard-Jones parameters (decreasing or increasing the van der Waals well depth for oxygen by up to 50 %), while preserving the agreement with ab initio energetics for small clusters. Results presented in this study are thus robust with respect to these force field modifications, with changes in observables not exceeding statistical noise.

In addition to the above straightforward MD simulations we employed the umbrella sampling technique[47] for obtaining free energy profiles of H_3O^+ and OH^- across the interface between water and a disordered alkane (icosane) monolayer. The icosane molecules in the monolayer have a tilt angle of approximately 30° and are arranged in a hexagonal lattice with a lattice constant appropriate for a gold (111) surface. The GAFF force field[44] is employed for icosane with atomic partial charges determined from an AM1 calculation and polarizabilities of its carbon and hydrogen atoms set to zero. After equilibration of the monolayer, all icosane atoms were harmonically restrained. More details on the construction of the icosane self-assembled monolayer are presented in Ref. 48.

The unit cell with dimensions of 30 x 34.6 x 90 Å contained 48 icosane molecules, 2000 POL3 waters, and a single hydronium or hydroxide ion. The same force field as above was employed for H_3O^+ and OH^-, with polarizability of hydroxide oxygen slightly reduced from 2.1 to 1.8 $Å^3$ to avoid possible instabilities of the very long simulations. A cutoff of 8 Å was was aplied to Lennard-Jones interactions, with long-range electrostatics being accounted for using PME.[42] Calculations were performend at 300 K and 1 atm.

For the umbrella sampling, the interfacial region was sampled in windows of width in the z-coordinate of 0.25 Å. For every window, a simulation was performed with a harmonic potential restraining the z-coordinate of the oxygen atom of the ion to the center of the

window. The force constant of the restraining potential was 2 kcal.mol^{-1}. Å^{-2}. Simulations were performed with a time step of 1 fs and the z-coordinate of the oxygen atom was saved every 50 fs. Next, the simulations were combined using the weighted histogram analysis method.[49] These calculations with a total simulation time of about 30 ns for each ion type were performed using the Amber 8 program package.[50]

Results and Discussion

The distributions of hydronium and hydroxide at the investigated interfaces are summarized in Figure 2. This composite picture shows density profiles along the direction perpendicular to the interface of individual species (i.e., hydronium, hydroxide, water, and carbon atoms) averaged over MD trajectories for the four investigated systems: i) water/disordered decane, ii) water/ordered decane, iii) water/rigid wall, and iv) water/vapor. The principal result emerging from these simulations is as follows: All of these interfaces attract hydronium cations (see large interfacial peaks of H_3O^+ in all plots in Figure 2) while there is no interfacial enhancement of hydroxide, save for the water/rigid wall system with a weak interfacial peak of OH^- (Figure 2c). This hydroxide peak correlates with strong water structuring and density fluctuations next to a rigid hydrophobic wall, as already described and discussed in previous studies.[40,51] Indeed, the three other, softer interfaces do not cause sizeable oscillations in water density and, consequently, do not appreciably surface segregate hydroxide (Figures 2abd). In contrast, the basic mechanism of surface enhancement of hydronium[12,14,23] is not tied to strong interfacial water structuring and density oscillations, therefore, it is operative for all investigated interfaces. Nevertheless, the rigid wall changes quantitatively the interfacial ion adsorption, making the hydronium peak narrower.

Interfacial water structuring is further analyzed, layer by layer, in terms of distributions of orientations θ of the water dipole (i.e., the oriented H-O-H angle bisector

pointing from the oxygen) with respect to the normal to the surface (Figure 3). All four interfaces orient water molecules in their vicinity, as demonstrated by non-uniform distribution of $cos\theta$. The distribution at the water/vapor interface (Figure 3d) agrees well with that obtained previously in a similar aqueous slab.[52] At the Gibbs dividing surface (GDS) and in its vicinity water dipoles lie preferentially parallel to the surface or slightly tilted into the gas phase. The water orientational distribution at the water/alkane interfaces is rather similar to that at the water/vapor interface, both in its peak position and width. In contrast, this distribution at the water/rigid wall interface is strikingly different. There is a sharp peak at $cos\theta = 0$ just below the GDS accompanied by several secondary peaks for varying values of $cos\theta$, which correlate with water density fluctuations. These results further underline the difference between the water/rigid wall interface from the three other, softer aqueous interfaces. Although even the soft aqueous interfaces can exhibit a certain degree of local water structuring and density fluctuations if the density is calculated as a function of a distance to the undulating soft surface, the structure of the aqueous solution just next to the interface is mostly determined by the character (rigidity and van der Waals attraction to water) of the surface.[53,54] Therefore, the differences in the structure of the interface between water and hard vs soft hydrophobic environments persist even if the analysis is done with respect to fluctuating surfaces.[55]

Next, we investigated orientations and free energy profiles of the ionic product of water at the interface between water and disordered alkane (icosane). The orientation of hydronium within the water/icosane interface is plotted in Figure 4, while that of hydroxide is shown in Figure 5. Distributions of $cos\theta$, where the angle is between the dipole of either of the ions and the normal to the surface, are plotted in layers parallel to the surface. These figures show quantitatively that H_3O^+ points its oxygen atom into the vapor, with maximum signal about 2 Å from the GDS toward the vapor phase. In contrast, OH^- tends to orient at the

interface with the hydrogen atom pointing into the vapor phase with the most oriented hydroxide anions residing right at the GDS.

The behavior of hydronium and hydroxide at the water/icosane interface was further investigated by evaluating the free energy profiles connected with moving either of these ions across the interface. The results are presented in Figure 6. For H_3O^+, we observe a sizable minimum at the potential of mean force in the region of the GDS with a depth of -2 kcal/mol. The potential of mean force for OH^- is much more flat. There is a very shallow (below kT) local free energy minimum about 1 Å from the GDS toward the aqueous bulk. Approximately 3 Å from the GDS, there is a shallow (again below kT) barrier to bulk solvation of hydroxide. Note that this weak structuring of the free energy profile of hydroxide nicely anticorrelates with small water density fluctuations (which are not observed at the water/vapor interface[9]).

Conclusions

We have investigated by means of molecular dynamics simulations the behavior of hydronium and hydroxide ions at the interface between water and alkane (ordered or disordered) or rigid wall or vapor. Qualitatively, all these interfaces exhibit a strong affinity for hydronium while there is at most a weak interfacial attraction of hydroxide. Quantitatively, the water/vapor and water/alkane interfaces behave similar to each other being, however, different from the water/rigid wall interface. When analysed with respect to GDS, the former interfaces are characterized by smooth water profiles with no (water/vapor) or weak (water/alkane) density oscillations. H_3O^+ exhibits a broad peak, while there is virtually no interfacial peak of OH^-. In contrast, the water/rigid wall interface is more structured with strong water density oscillations. Consequently, the interfacial peak of hydronium is narrower and higher than in the other investigated cases and there appears a weak interfacial peak of hydroxide.

The observed adsorption of hydronium at water/vapor or water/alkane interfaces is consistent both with surface selective spectroscopy[2,22-24] and with zeta-potential measurements at low pH of air bubbles and oil droplets in water.[29,56] The lack of appreciable surface adsorption of OH^- in the present simulations is supported by recent surface selective spectroscopic measurements at the water/vapor for a broad range of hydroxide concentrations (from zero to several moles).[2,22,25,26] These results are, however, at odds with the interpretation of higher pH zeta-potential and titration measurements, as well as thin film experiments, in terms of strong adsorption of hydroxide at the water/vapor or water/oil interfaces.[30-32,36,37]

Acknowledgment

Support (to P.J.) from the Czech Ministry of Education (grant LC512) and the Czech Science Foundation (grant 203/08/0114). R.V. acknowledges support from the Czech Science Foundation (grant 203/05/H001) and from the International Max-Planck Research School.

References

[1] *For a recent review see, e.g.,* Jungwirth, P.; Tobias, D. J.; Finlayson-Pitts, B. J. *Chem. Rev.* **2006**, *106*, 1137.

[2] Gopalakrishnan, S.; Liu, D. F.; Allen, H. C.; Kuo, M.; Shultz, M. J. *Chem. Rev.* **2006**, *106*, 1155.

[3] Winter, B.; Faubel, M. *Chem. Rev.* **2006**, *106*, 1176.

[4] Raymond, E. A.; Richmond, G. L. *J. Phys. Chem. B* **2004**, *108*, 5051.

[5] Petresen, P. B.; Saykally, R. J. *Chem. Phys. Lett.* **2004**, *397*, 51.

[6] Luo, G.; Malkova, S.; Yoon, J.; Schultz, D. G.; Lin, B.; Meron, M.; Benjamin, I.; Vanysek, P.; Schlossman, M. L. *Science* **2006**, *311*, 216.

[7] Chang, T. M.; Dang, L. X. *Chem. Rev.* **2006**, *106*, 1322.

[8] Jungwirth, P.; Tobias, D. J. *Chem. Rev.* **2006**, *106*, 1259.

[9] Vacha, R.; Buch, V.; Milet, A.; Devlin, J. P.; Jungwirth, P. *Phys. Chem. Chem. Phys.* **2007**, *9*, 4736.

[10] Beattie, J. K. *Phys. Chem. Chem. Phys.* **2008**, *10*, 330.

[11] Vacha, R.; Buch, V.; Milet, A.; Devlin, J. P.; Jungwirth, P. *Phys. Chem. Chem. Phys.* **2008**, *10*, 332.

[12] Petersen, M. K.; Iyengar, S. S.; Day, T. J. F.; Voth, G. A. *J. Phys. Chem. B* **2004**, *108*, 14804.

[13] Dang, L. X. *J. Chem. Phys.* **2003**, *119*, 6351.

[14] Mucha, M.; Frigato, T.; Levering, L. M.; Allen, H. C.; Tobias, D. J.; Dang, L. X.; Jungwirth, P. *J. Phys. Chem. B* **2005**, *109*, 7613.

[15] Swanson, J. M. J.; Mauphin, C. M.; Chen, H.; Petersen, M. K.; Xu, J.; Wu, Y.; Voth, G. A. *J. Phys. Chem. B* **2007**, *111*, 4300.

[16] Buch, V.; Milet, A.; Vacha, R.; Jungwirth, P.; Devlin, J. P. *Proc. Natl. Acad. Sci USA* **2007**, *104*, 7342.

[17] Eigen, M. *Angewandte Chem., Int. Ed.* **1964**, *3*, 1.

[18] Zundel, G. *Adv. Chem. Phys.* **2000**, *111*, 1.

[19] Tuckerman, M. E.; Chandra, A.; Marx, D. *Acc. Chem. Res.* **2006**, *39*, 1511.

[20] Megyes, T.; Balint, S.; Grosz, T.; Radnai, T.; Bako, I.; Sipos, P. *J. Chem. Phys.* **2008**, *128*, 044501.

[21] Aziz, E. F.; Ottosson, N.; Faubel, M.; Hertel, I. V.; Winter, B. *submitted.*

[22] Tarbuck, T. L.; Ota, S. T.; Richmond, G. L. *J. Am. Chem. Soc.* **2006**, *128*, 14519.

[23] Petersen, P. B.; Saykally, R. J. *J. Phys. Chem. B* **2005**, *109*, 7976.

[24] Petersen, P. B.; Saykally, R. J. *Annu. Rev. Phys. Chem.* **2006**, *57*, 333.

[25] Petersen, P. B.; Saykally, R. J. *Chem. Phys. Lett., submitted.*

[26] Vacha, R.; Winter, B.; Faubel, M.; Jungwirth, P. *to be submitted.*

[27] Gilbert, H. W.; Shaw, P. E. *Proc. Phys. Soc. London* **1924**, *37*, 195.

[28] Graciaa, A.; Morel, G.; Saulner, P.; Lachaise, J.; Schechter, R. S. *J. Colloid Interface Sci.* **1995**, *172*, 131.

[29] Takahashi, M. *J. Phys. Chem. B* **2005**, *109*, 21858.

[30] Marinova, K. G.; Alargova, R. G.; Denkov, N. D.; Velev, O. D.; Petsev, D. N.; Ivanov, I. B.; Borwankar, R. P. *Langmuir* **1996**, *12*, 2045.

[31] Beattie, J. K.; Djerdjev, A. M. *Angew. Chem. Int. Ed.* **2004**, *43*, 3568.

[32] Beattie, J. K. *Lab Chip* **2006**, *6*, 1409.

[33] Beattie, J. K. *in: Colloid Stability: The Role of Surface Forces, Part II,* ed. Tadros, T. F., Wiley, Weinheim, 2006, p. 153.

[34] Maze, J. T.; Zilch, L. W.; Smith, J. W.; Ewing, G. E.; Jarrold, M. F. *submitted*.

[35] Bergeron, V.; Waltermo, A.; Claesson, P. M. *Langmuir* **1996**, *12*, 1336.

[36] Karraker, K. A.; Radke, C. J. *Adv. Colloid Interface Sci.* **2002**, *96*, 231.

[37] Stubenrauch, C; von Klitzing, R. *J. Phys.-Condensed Matter* **2003**, *15*, R1197.

[38] Koelsch, P.; Viswanath, P.; Motschmann, H.; Shapovalov, V. L.; Brezesinski, G.; Mohwald, H.; Horinek, D.; Netz, R. R.; Giewekemeyer, K.; Salditt, T.; Schollmeyer, H.; von Klitzing, R.; Daillant, J.; Guenoun, P. *Colloids Surf. A* **2007**, *303*, 110.

[39] Zangi, R.; Engberts, J. B. F. N. *J. Am. Chem. Soc.* **2005**, *127*, 2272.

[40] Vacha, R.; Zangi, R.; Engberts, J. B. F. N.; Jungwirth. P. *J. Phys. Chem. C, in press.*

[41] Lindahl, E.; Hess, B.; van der Spoel, D. *J. Mol. Model.* **2001,** *7,* 306.

[42] Essmann, U.; Perera, L.; Berkowitz, M. L.; Darden, T.; Lee, H.; Pedersen, L. G. *J. Chem. Phys.* **1995**, *103*, 8577.

[43] Caldwell, J. W.; Kollman, P. A. *J. Phys. Chem.* **1995**, *99*, 6208.

[44] Wang, J. M.; Wolf, R. M.; Caldwell, J. M.; Kollman, P. A.; Case, D. A. *J. Comput. Chem.* **2004**, *25*, 1157.

[45] Singh, U. C.; Kollman, P. A. *J. Comput. Chem.* **1984**, *5*, 129.

[46] Botti, A.; Bruni, F.; Imberti, S.; Ricci. M. A.; Soper, A. K. *J. Chem. Phys.* **2004**, *120*, 10154.

[47] Torrie, G.; Valleau, J. *J. Comp. Phys.* **1977**, *23*, 187.

[48] Horinek, D.; Netz R. R. *Phys. Rev. Lett.* **2007**, *99*, 226104.

[49] Kumar, S.; Boudzida, D.; Swendsen, R. H.; Kollman, P. A.; Rosenberg J. M. *J. Comp. Chem.* **1992**, *13*, 1011.

[50] Case, D. A.; Darden, T. A.; Cheatham, III, T. E.; Simmerling, C. L.; Wang, J.; Duke, R. E.; Luo, R.; Merz, K. M.; Wang, B.; Pearlman, D. A.; Crowley, M.; Brozell, S.; Tsui, V.; Gohlke, H.; Mongan, J.; Hornak, V.; Cui, G.; Beroza, P.; Schafmeister, C.; Caldwell, J. W.; Ross, W. S.; Kollman, P.A. *AMBER 8*, University of California, San Francisco, 2004.

[51] Jensen, M. O.; Mouritsen, O. G.; Peters, G. H. *J. Chem. Phys.* **1995**, *120*, 9729.

[52] Brown, E. C.; Mucha, M.; Jungwirth, P.; Tobias, D. J. *J. Phys. Chem. B* **2005**, *109*, 7934.

[53] Pandit, S. A.; Bostick, D.; Berkowitz, M. L. *J. Chem. Phys.* **2003**, *119*, 2199.

[54] Bhide, S. Y.; Berkowitz, M. L. *J. Chem. Phys.* **2005**, *123*, 224702.

[55] Chowdhary, J.; Ladanyi, B. M. *J. Phys. Chem. B* **2006**, *110*, 15442.

[56] Zimmermann, R.; Dukhin, S.; Werner, C. *J. Phys. Chem. B* **2001**, *105*, 8544.

Figure captions:

Figure 1: Snapshots showing the investigated interfaces. a) water/disordered decane, b) water/ordered decane, c) water/rigid wall, and d) water/vapor. Color coding: oxygen atoms – blue, hydrogen atoms – white, and carbon atoms – gold.

Figure 2: Number density profiles of individual species along the z-direction perpendicular to the interface, averaged over the simulations. All ion profiles were normalized in the same way with intergrals under the density profiles equal to that of water. Each plot is a summary of two simulations, one with H_3O^+ and the other with OH^-. Distances are plotted with respect to the Gibbs dividing surface. a) water/disordered decane, b) water/ordered decane, c) water/rigid wall, and d) water/vapor.

Figure 3: Orientation of water molecules in layers parallel to the hydrophobic interface, i.e, distribution of cosines of angles θ between the water dipole and the normal to the interface, represented in a color scheme. Distances are plotted with respect to the Gibbs dividing surface. a) water/disordered decane, b) water/ordered decane, c) water/rigid wall, and d) water/vapor.

Figure 4: Orientation of the hydronium cation in layers parallel to the water/icosane interface, i.e, distribution of cosines of angles θ between the ion dipole and the normal to the interface, represented in a color scheme. Distances are plotted with respect to the Gibbs dividing surface.

Figure 5: Orientation of the hydroxide anion in layers parallel to the water/icosane interface, i.e, distribution of cosines of angles θ between the ion dipole and the normal to the interface, represented in a color scheme. Distances are plotted with respect to the Gibbs dividing surface.

Figure 6: Potentials of mean force (i.e., free energy profiles along the z-coordinate perpendicular to the interface) for of H_3O^+ and OH^- at the water/icosane interface. Zero coordinate value corresponds to the Gibbs dividing surface. Depicted is the H_3O^+ potential of mean force (red), the OH^- potential of mean force (green) and the water density profile (blue). The prefered orientation of each of the ions at the inetrface is also shown.

Figure 1

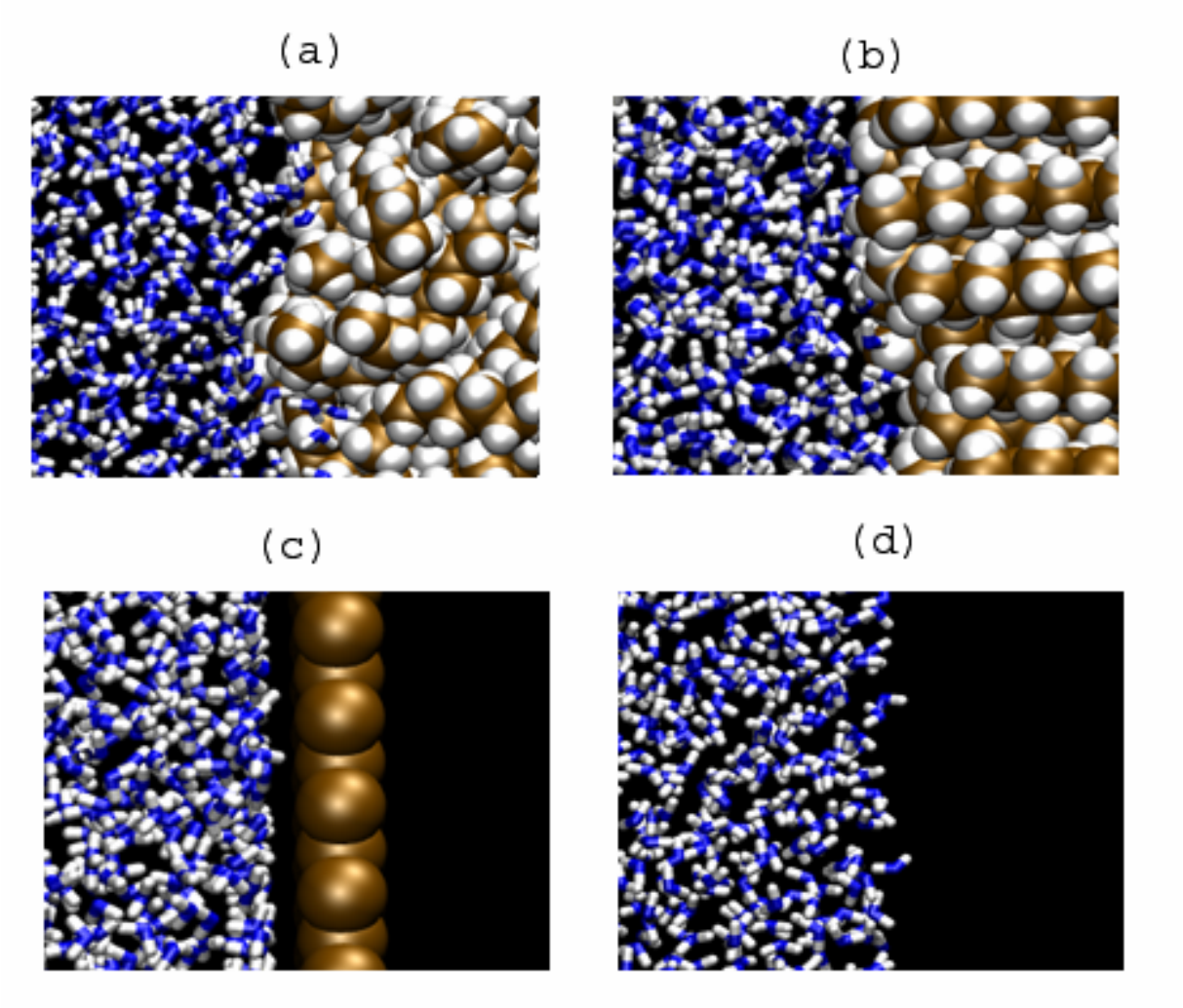

Figure 2

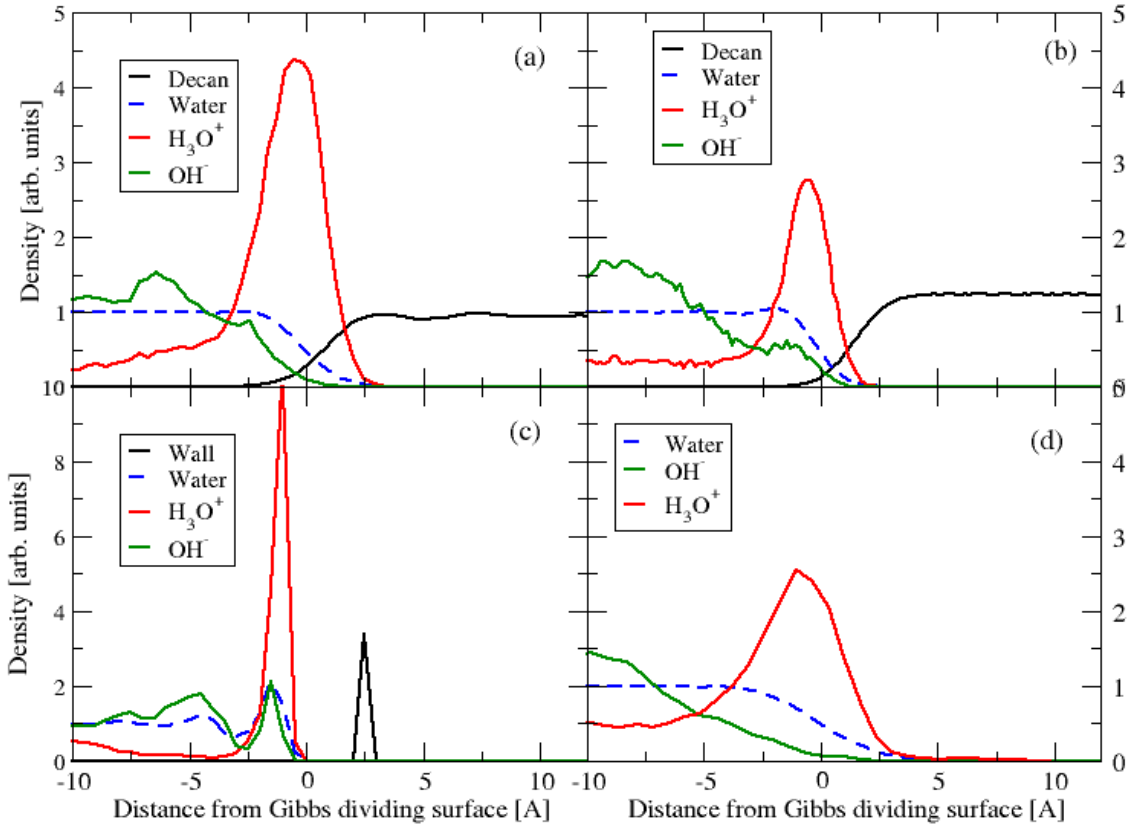
(a)
Decan
Water
H_3O^+
OH^-
(b)
Decan
Water
H_3O^+
OH^-
(c)
Wall
Water
H_3O^+
OH^-
(d)
Water
OH^-
H_3O^+
Density [arb. units]
Density [arb. units]
Distance from Gibbs dividing surface [A]
Distance from Gibbs dividing surface [A]

Figure 3:

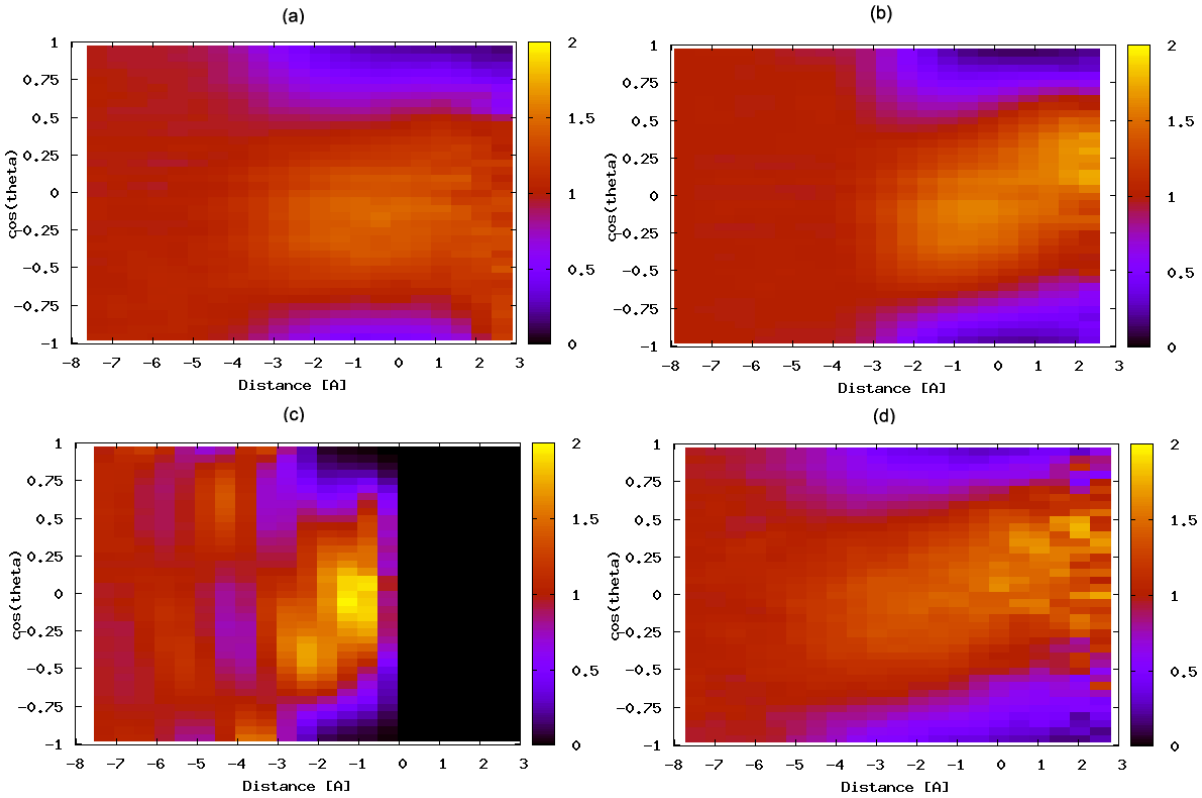

Figure 4

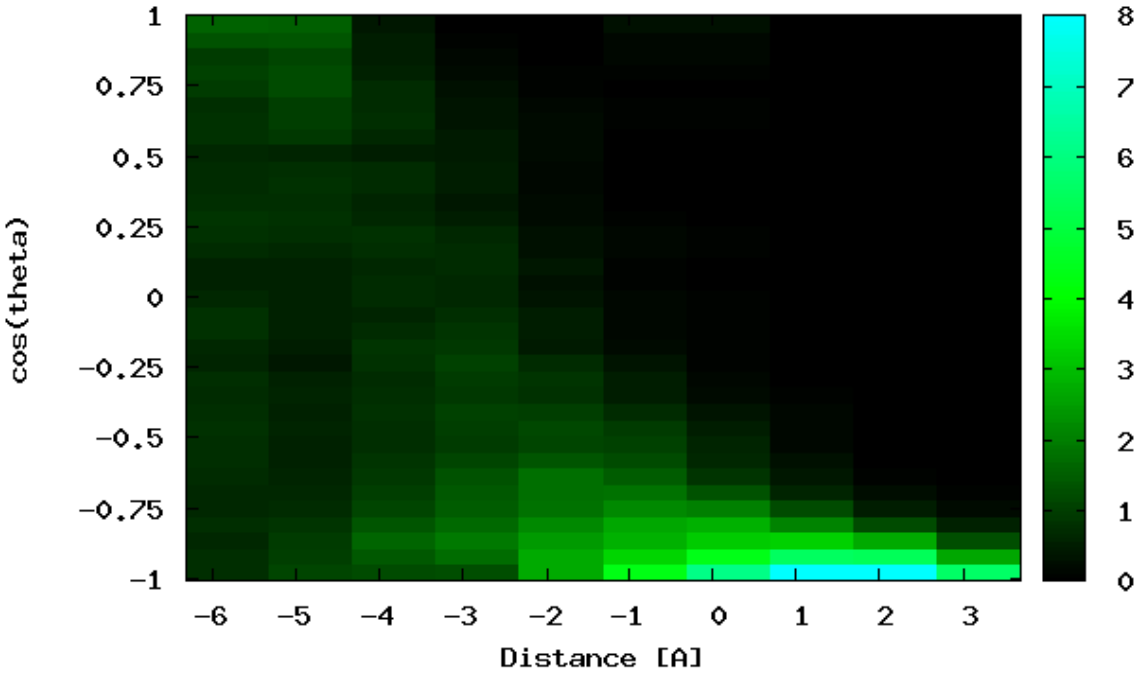
cos(theta)
1
0.75
0.5
0.25
0
-0.25
-0.5
-0.75
-1
-6
-5
-4
-3
-2
-1
0
1
2
3
Distance [A]
8
7
6
5
4
3
2
1
0

Figure 5:

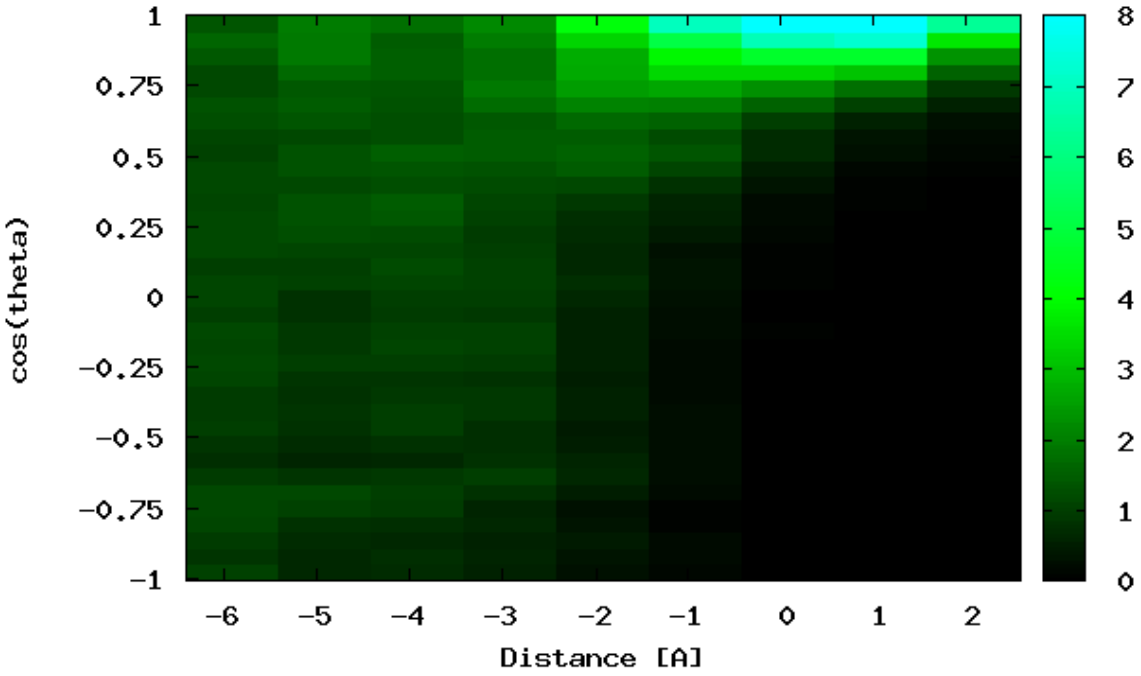
cos(theta)
1
0.75
0.5
0.25
0
-0.25
-0.5
-0.75
-1
-6
-5
-4
-3
-2
-1
0
1
2
Distance [A]
8
7
6
5
4
3
2
1
0

Figure 6:

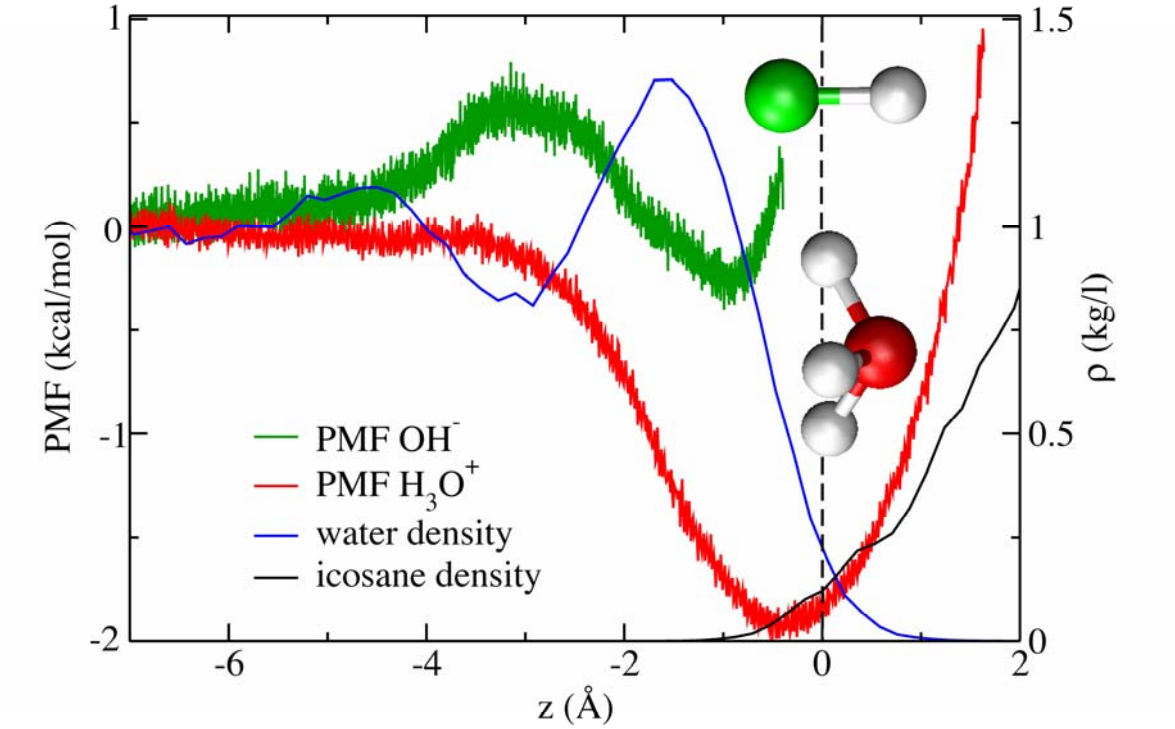
PMF (kcal/mol)
ρ (kg/l)
z (Å)
PMF OH-
PMF H3O+
water density
icosane density
1
0
-1
-2
1.5
1
0.5
0
-6
-4
-2
0
2